Neurotox Res (2015) 27:143–155
DOI 10.1007/s12640-014-9492-x

ORIGINAL ARTICLE

3,4-Dihydroxyphenylethanol Attenuates Spatio-Cognitive Deficits in an Alzheimer's Disease Mouse Model: Modulation of the Molecular Signals in Neuronal Survival-Apoptotic Programs

Mohanasundaram Arunsundar · Thukani Sathanantham Shanmugarajan · Velayutham Ravichandran

Received: 27 July 2014 / Revised: 1 September 2014 / Accepted: 8 September 2014 / Published online: 2 October 2014

Abstract Alzheimer's disease (AD), the most common type of dementia, is a devastating neurodegenerative disease characterized by progressive neuro-cognitive dysfunction. In our study, we investigated the potential of 3,4-dihydroxyphenylethanol (DOPET), a dopamine metabolite, and also a polyphenol from olive oil, in ameliorating soluble oligomeric amyloid β_{1-42} plus ibotenic acid (oA42i)-induced neuro-behavioral dysfunction in C57BL/6 mice. The results depicted that intracerebroventricular injection of oA42i negatively altered the spatial reference and working memories in mice, whereas DOPET treatment significantly augmented the spatio-cognitive abilities against oA42i. Upon investigation of the underlying mechanisms, oA42i-intoxicated mice displayed significantly activated death kinases including JNK- and p38-MAPKs with concomitantly inhibited ERK-MAPK/RSK2, PI3K/Akt1, and JAK2/STAT3 survival signaling pathways in the hippocampal neurons. Conversely, DOPET treatment reversed these dysregulated signaling mechanisms comparable to the sham-operated mice. Notably, oA42i administration altered the Bcl-2/Bad levels and activated the caspase-dependent mitochondria-mediated apoptotic pathway involving cytochrome *c*, apoptotic protease activating factor-1, and caspase-9/3. In contrary, DOPET administration stabilized the dysregulated activities of these apoptotic/anti-apoptotic markers and preserved the mitochondrial ultra-architecture. Besides, we observed that oA42i intoxication substantially down-regulated the expression of genes involved in the regulation of survival and memory functions including sirtuin-1, cyclic AMP response element-binding protein (CREB), CREB-target genes (BDNF, c-*Fos*, *Nurr1*, and *Egr1*) and a disintegrin and metalloprotease 10. Fascinatingly, DOPET treatment significantly diminished these aberrations when compared to the oA42i group. Taken together, these results accentuate that DOPET may be a multipotent agent to combat AD.

Keywords DOPET · Alzheimer's disease · Apoptosis · $A\beta_{1-42}$ oligomer · MAPK · CREB

M. Arunsundar · T. S. Shanmugarajan (✉)
Department of Pharmacology, School of Pharmaceutical Sciences, Vels University, Pallavaram, Chennai 600117, India
e-mail: shanmuga5@yahoo.com

V. Ravichandran
Department of Pharmacognosy, School of Pharmaceutical Sciences, Vels University, Pallavaram, Chennai 600117, India

Introduction

The pathognomonic signs of Alzheimer's disease (AD) are extracellular senile plaques with amyloid-beta (Aβ) peptide deposits and intracellular neurofibrillary tangles with hyperphosphorylated microtubule-associated tau-protein aggregates which cause neuronal stress and neuronal circuit disruption, eventually culminating in neurodegeneration and brain atrophy (Praticò 2013). Although the "*primum movens*" of AD is remaining obscure, many reports underscore the causal link between perturbed neuronal death-survival equilibrium and neuro-behavioral dysfunction in AD (Fiocchetti et al. 2013; Godoy et al. 2014).

The "Aβ oligomer hypothesis" has supplanted the "amyloid cascade hypothesis" as the former seems to fill the lacuna in correlating amyloid plaque deposits and memory impairment or neuronal injury (Benilova et al. 2012). According to the widely accepted "Aβ oligomer hypothesis", soluble neurotoxic Aβ oligomers play a

pivotal role in AD pathogenesis and the Aβ oligomers accelerate a plethora of noxious cellular and sub-cellular events in the brain including calcium dyshomeostasis, excitotoxicity, neuroinflammation, ER stress, cytoskeletal collapse, mitochondrial damage and fragmentation, neurosynaptic dysfunction, and accelerated apoptosis—ultimately leading to nerve cell demise and cognitive dysfunction (Benilova et al. 2012; Kayed and Lasagna-Reeves 2013).

Most researchers advocate that extracellular signal-regulated kinase-mitogen-activated protein kinase (ERK-MAPK), phosphoinositide-3-kinase/Akt (PI3K/Akt) and Janus kinase 2/signal transducer and activator of transcription 3 (JAK2/STAT3) signaling are the crucial survival pathways impaired in the Alzheimer's disease (Kawamata and Shimohama 2011; Marwarha and Ghribi 2012). Thus, activation of these pathways might rescue the AD brain from learning and memory impairments. Recently, Denner et al. (2012) reported that hippocampal ERK2 is a central regulator of learning and memory functions. This study is in sync with the report of Satoh et al. (2007) on ERK2 knock-down mice, which displayed long-term memory deficits. Besides, there are substantial reports on the amyloid β-induced impairment of PI3K/Akt1 and JAK2/STAT3 axes which in turn caused hippocampus-linked memory dysfunctions (Chiba et al. 2009; Liao and Xu 2009).

Based on the recent reviews and research studies on both clinical and experimental AD models, we conjecture that synchronized regulation of various neuromolecular switches—involved in the neuronal apoptosis and survival signaling pathways—might confer protection against the pathogenesis of beta-amyloid-induced brain cell damage and memory deficiency (Fiocchetti et al. 2013; Godoy et al. 2014; Nehlig 2013; Tan et al. 2012). Thus, an exemplar anti-Alzheimer's drug must possess dual multipotency to counteract the toxic episodes and enhance the declined neuro-behavioral functions in AD.

3,4-Dihydroxyphenylethanol (DOPET; hydroxytyrosol) is a biophenol present in olive oil, wine, grape juice and notably, it is an endogenous metabolite of dopamine (de la Torre et al. 2006). Beyond its high safety index (Auñon-Calles et al. 2013), DOPET has been reported to exhibit central and peripheral neuroprotective (González-Correa et al. 2008; Ristagno et al. 2012), cardioprotective (Granados-Principal et al. 2014), uroprotective (Rouissi et al. 2011), nephroprotective (Capasso et al. 2008), hepatoprotective (Pan et al. 2013), anti-diabetic and anti-obesity (Cao et al. 2014), anti-osteoporotic (Hagiwara et al. 2011), anti-inflammatory (de la Puerta et al. 1999), anti-atherosclerotic (González-Santiago et al. 2006), anti-cancer (Zhao et al. 2014), and anti-HIV effects (Lee-Huang et al. 2007). Fascinatingly, St-Laurent-Thibault et al. (2011) showed that DOPET offers protection against amyloid β-induced neurotoxicity in N2a cells. Moreover, DOPET was reported to exert Tau anti-fibrillization effect in vitro (Daccache et al. 2011). With this backdrop of research reports, we hypothesized that DOPET may be a putative multipotent anti-Alzheimer's agent. As far as we are aware, this is the first report to elucidate the molecular mechanisms involved in the neuroprotective and cognition-enhancing effect of DOPET in an in vivo AD model.

Materials and Methods

Drugs and Animals

DOPET (≥98 %) (Fig. 1a) and synthetic Aβ-(1–42) peptide (Fig. 1b) were purchased from Extrasynthese (Genay Cedex, France) and American Peptide Co., (Sunnyvale, CA) respectively. Ibotenic acid (Fig. 1c) was purchased from Abcam (Cambridge, UK). Thirty adult male C57BL/6 mice, aged 6–8 weeks and weighing 20–25 g, were housed in temperature- and humidity-controlled animal quarters under 12-h light/12-h dark cycles. The light/dark cycle corresponded to the timing of lights on at 07:00 a.m. (IST) and to the timing of lights off at 07:00 p.m. (IST), respectively. The animals had access to food and water ad libitum. Each mouse was handled for 5 min/day on three consecutive days, starting 2 days after arrival, before being subjected to the study. All experiments were conducted in accordance with animal care guidelines approved by the Institutional Animal Ethics Committee (IAEC) of the Vels University.

Fig. 1 Structure/amino acid sequence of compounds

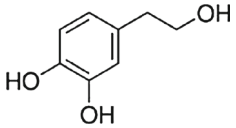

A DOPET

Asp-Ala-Glu-Phe-Arg-His-Asp-Ser-Gly-Tyr-Glu-Val-His-His-Gln-Lys-Leu-Val-Phe-Phe-Ala-Glu-Asp-Val-Gly-Ser-Asn-Lys-Gly-Ala-Ile-Ile-Gly-Leu-Met-Val-Gly-Gly-Val-Val-Ile-Ala

B $A\beta_{1-42}$ peptide

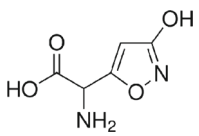

C Ibotenic acid

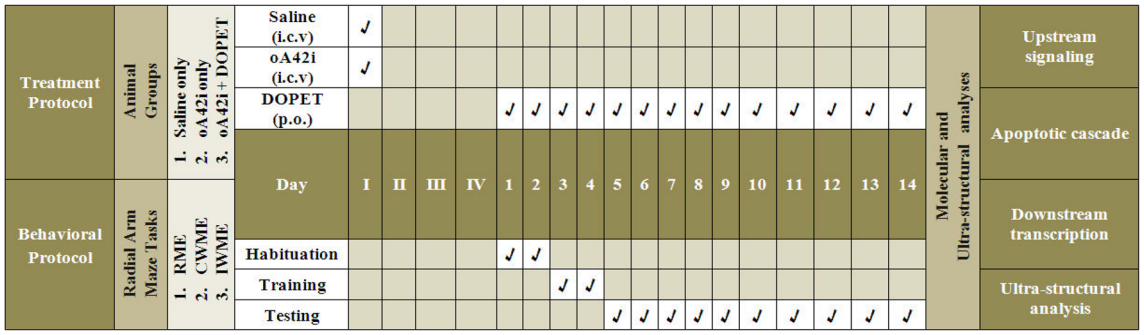

Fig. 2 Study design

Surgery and Treatment Protocol

Neurodegeneration was induced in mice, based on the model proposed by Morimoto et al. (1998) with minor modifications. Briefly, mice were deeply anesthetized by injecting ketamine (100 mg/kg, i.p.) and xylazine (10 mg/kg, i.p.) and the surgical site was shaved and sterilized. An incision roughly 1.5 cm in length was made on the cranium to reveal the bregma. On day I (by 7 a.m.), each anesthetized mouse was mounted in a stereotaxic apparatus and one microliter of each neurotoxicant solution (oA42i; soluble $oA\beta_{1-42}$, and ibotenic acid-in-PBS) was injected over 5 min through a 26-gauge Hamilton syringe into the lateral ventricle [−0.6 mm anterior–posterior (AP), 1.2 mm medial–lateral (ML), and −2 mm dorsal–ventral (DV)], relative to the bregma (Paxinos and Franklin 2001). Mice in the sham-operated group were administered with the same volume of sterile saline in the similar fashion. The needle was slowly withdrawn from the site of injection only after 5 min to prevent any backflow. One hour after the i.c.v. injection of sterile saline or oA42i (oligomeric $A\beta_{1-42}$ plus ibotenic acid), all the thirty mice were randomly allocated to one of the three groups and treated as follows (Fig. 2): saline-injected sham-operated group, oA42i-injected group, and oA42i-injected DOPET treatment group. After 4 days of recovery period (day I-IV), the animals in DOPET group were administered sub-chronically with DOPET [10 mg/(kg day), p.o.] for 14 days by oral gavage, regularly by 7 a.m. Also, 6 h after DOPET administration, animals in all the three groups were subjected to RAM exposure from day 1 to day 14 as portrayed in Fig. 2.

Preparation of Aβ Oligomers

Amyloid beta oligomers were prepared from $A\beta_{1-42}$ peptide as described by Klein (2002). In brief, the $A\beta_{1-42}$ peptide, previously chilled on ice, was solubilized in ice-cold hexafluoroisopropanol (HFIP, Sigma–Aldrich Pvt. Ltd., India) to disintegrate any pre-existing aggregates and a final concentration of 1 mM was made. Then, the Aβ-HFIP solution was incubated at room temperature for 1 h in a closed vial and again the solution was placed back on ice for about 10 min. The solution was vortexed and aliquoted into Eppendorf microcentrifuge tubes and left overnight in the hood at room temperature to allow HFIP evaporation. After lyophilization, the obtained dry monomeric films of $A\beta_{1-42}$ peptide were stored over desiccant at −80 °C. Aβ monomer preparations were prepared in situ to curtail potential aggregation of peptide. For the oligomer preparation, the dried peptide was re-suspended in anhydrous dimethyl sulfoxide (DMSO, Merck India Ltd., India) to make a 5 mM stock. The resultant solution was additionally diluted to 100 μM in phenol red-free Ham's F-12 medium, immediately vortexed for 30 s, and incubated for 24 h at 5 °C. The preparation was centrifuged at $14{,}000 \times g$ for 10 min at 4 °C to pellet out insoluble aggregates (protofibrils and fibrils), and the supernatants containing soluble neurotoxic Aβ-oligomers (also called ADDLs; Aβ-derived diffusible ligands) were transferred to a new tube and stored at 4 °C for further use.

Behavioral Assessment

Apparatus

Spatial reference and working memories were assessed using a radial arm maze (RAM), as reported by Brown et al. (2002) with minor modifications. Briefly, the apparatus was designed with eight identical and equally spaced arms (25 cm long × 8.5 cm wide) radiating from a central octagonal platform (25 cm in diameter) with a recessed food cup (1 cm from the end and 1.5 cm deep). The RAM apparatus was elevated to a height of 30 cm from the ground and placed in a small, well-lit room that contained a number of visual cues. At the entrance to each arm was a door that could be controlled using strings.

Habituation Phase

The behavioral assessment was carried out as shown in Fig. 2. Every exposure of a mouse to the maze at any phase is designated as a trial. During habituation phase, food baits (Kellogg's Chocos Duet® Snacks) were scattered throughout the maze to encourage exploration and to lessen fear and anxiety of mice from exposure to the strange maze setting. The residence time of the mice was restricted to 5 min during each exploration and there were two trials on each day. Throughout the behavioral assessment, the maze was cleaned using paper towels dampened in ethanol (70 %) to remove the traces of urine and feces and to exclude any olfactory cue, at the end of every trial.

Training Phase

During training period, only single food bait was placed down in each of the 8 arms of RAM. Mice were released on the central platform and allowed to travel around all the 8 arms. Mice remained on the maze for 5 min during each training trial. The observations in both habituation and training phases were not recorded as these phases are mainly meant to lessen the experimental errors in testing phase.

Testing Phase

In the testing phase, mice were tested for the spatial reference and working memory performances for 10 consecutive days with one trial per day. Four arms (2, 3, 5, and 7) were randomly baited with food reward so that no more than one pair of adjacent arms was baited or unbaited. This paradigm was maintained steadily till the end of the assessment. The trial was terminated when all of the baits were consumed or 5 min had passed, whichever was earlier.

Error Recording

Three types of errors were scored: reference memory errors (RME), defined as the number of first entries into an unbaited arm; "correct" working memory errors (CWME), defined as the number of reentries into a baited arm and "incorrect" working memory errors (IWME), defined as the number of reentries into an unbaited arm (Schmitt et al. 2003).

Tissue Harvesting

On the 15th day, all the mice were sacrificed by cervical dislocation, their brains were rapidly excised, and the hippocampi were dissected out on ice, then snap frozen in liquid nitrogen, and kept at −80 °C until analyzed.

Western Blot Analysis

The hippocampi were chopped into small pieces and about 5 mg of the tissue was transferred to microcentrifuge tubes. Then, 300 µl of the cell lysis buffer—cold RIPA (radioimmunoprecipitation assay) buffer (Abcam, Cambridge, UK) containing 0.22 % beta glycerophosphate, 10 % tergitol-NP40, 0.18 % sodium orthovanadate, 5 % sodium deoxycholate, 0.38 % EGTA, 1 % SDS, 6.1 % Tris, 0.29 % EDTA, 8.8 % sodium chloride, 1.12 % sodium pyrophosphate decahydrate (pH 7.5)—was added to the tubes and homogenized with an electric homogenizer and the blades were rinsed twice with the same volume of lysis buffer. The lysate was placed in an orbital shaker for 2 h at 4 °C. Then, the solubilized proteins were collected from the supernatant after centrifugation at 16,000×*g* for 20 min at 4 °C and the debris was discarded. A small volume (50 µl) of the lysate was taken to determine protein concentration using protein assay reagent (Bio-Rad Laboratories, Hercules, CA). Equal amount of proteins (30 µg) were separated on SDS–polyacrylamide gels with a Tris–glycine/SDS running buffer system and then transferred to a polyvinylidene difluoride (PVDF) membrane (Millipore, Billerica, MA). After blocking in 5 % non-fat milk in Tris-buffered saline containing 0.1 % Tween-20 (TBST), the membranes were incubated overnight at 4 °C with specific primary antibodies: anti-Akt1 and anti-phospho-Ser473-Akt1 (1:1,000, Cell Signaling Technology, Inc. Danvers, MA), anti-ERK1/2 and anti-phospho-Thr202/Tyr204-ERK1/2 (1:1,000, Santa Cruz Biotechnology, Inc., CA), anti-RSK2 and anti-phospho-Thr577-RSK2 (1:1,000, Santa Cruz Biotechnology, Inc., CA), anti-JAK2 and anti-phospho-Tyr1007/1008-JAK2 (1:1,000, Cell Signaling Technology, Inc. Danvers, MA), anti-STAT3 and anti-phospho-Tyr705-STAT3 (1:1,000, Cell Signaling Technology, Inc. Danvers, MA), anti-JNK and anti-phospho-Thr183-JNK (1:1,000, Santa Cruz Biotechnology, Inc., CA), anti-p38 and anti-phospho-Thr180/Tyr182-p38 (1: 2,000, Cell Signaling Technology, Inc. Danvers, MA), anti-CREB and anti-phospho-Ser133-CREB (1:1,000, Millipore, Billerica, MA), anti-SIRT1 (1:1,000, Santa Cruz Biotechnology, Inc., CA) and anti-ADAM10 (1:1,000, Abcam, Cambridge, UK). After washing, the membranes were then incubated with secondary horseradish peroxidase-conjugated antibodies (Santa Cruz Biotechnology, Inc., CA) and visualized with chemiluminescence reagents provided with the ECL (enhanced chemiluminescent) kit (Abcam, Cambridge, UK). The intensity of chemiluminescent bands was measured using Quantity One® software (Bio-Rad).

RNA Isolation and RT-PCR Assay

For the RT-PCR assay, total RNA was extracted by using RNeasy® total RNA isolation kit (Qiagen, Valencia, CA). Briefly, 10 mg of the chopped hippocampal tissues was disrupted and homogenized by using lysis buffer (350 µl) and the lysate was centrifuged at 16,000×*g* for 3 min and processed further to yield 10 µg RNA. The cDNA was synthesized from RNA using the SuperScript® One-Step RT-PCR kit (Invitrogen). The Thermal Cycler 2400 (Perkin Elmer) was programed so that cDNA synthesis follows immediately with PCR amplification, automatically. The amplified products were separated by electrophoresis on a 2 % agarose gel containing ethidium bromide and photographed. Band intensities were determined by an image analysis system (Alpha Imager gel documentation system, CA). The following are the primers used in the RT-PCR assay: β-actin: sense 5′-TCTTGGGTATGGAATCCTGTG-3′ and antisense 5′-ATCTCCTTCTGCATCCTGTCA-3′; cytochrome *c*: sense 5′-ATAGGGGCATGTCACCTCAAAC-3′ and antisense 5′-GTGGTTAGCCATGACCTGAAAG-3′; Caspase-9: sense 5′-GTGGACATTGGTTCTGGC-3′ and antisense 5′-GTTGATGATGAGGCAGTGG-3′; Apaf-1: sense 5′-TTGATGCTGTCATTATGTAGGC-3′ and antisense 5′-AGGTAAAAGGGGAAGTATGTGTT-3′; Caspase 3: sense 5′-TCTTCATCATTCAGGCCTG-3′ and antisense 5′-TGAATTTCTCCAGGAATAGTAACC-3′; Bcl-2: sense 5′-CTGGGATGCCTTTGTGGAAC-3′ and antisense 5′-TCAAACAGAGGTCGCATGCT-3′; Bad: sense 5′-CCAGTGATCTTCTGCTCCACATCCC-3′ and antisense 5′-CAACTTAGCACAGGCACCCGAGGG-3′; BDNF: sense 5′-AGGCACTGGAACTCGCAATG-3′ and antisense 5′-AAGGGCCCGAACATACGATT-3′; c-*Fos*: sense 5′-GATGTTCTCGGGTTTCAACG-3′ and antisense 5′-GGAGAAGGAGTCGGCTGG-3′; *Nurr1*: sense 5′-AGTACCTTTATGGACAACTACAGCA-3′ and antisense 5′-CGTAGTGGCCACGTAGTTCTGGT-3′; *Egr1*: sense 5′-CCCTGTGCCCACTTCCTACTCCT-3′ and antisense 5′-CGGCCATCTCTTCCCTCCTGT-3′.

Transmission Electron Microscopy (TEM)

The TEM study was performed according to the method of Hajibagheri (1999). Briefly, the hippocampi were chopped and fixed with 2.5 % glutaraldehyde in 0.1 M cacodylate buffer. The fixed tissues were post-fixed in 1 % osmium tetroxide for 1 h at RT and then dehydrated in an ethanol series. Then, the slices were infiltrated and embedded in epoxy resins. Ultrathin sections of 800 Å were cut using ultramicrotome (LKB Ultratome, NOVA). The grids containing sections were stained with 2 % uranyl acetate followed by Reynolds lead citrate. Grids were examined and photographed under JEM-2010 transmission electron microscope (JEOL Ltd, Tokyo, Japan).

Statistical Analysis

The data were represented as the mean ± standard deviation (SD). Two-way analysis of variance (ANOVA) was applied for behavioral assessment (RAM tasks). One-way ANOVA was applied for biochemical evaluations. In this study, Tukey's post-hoc test was used as a measure of between-group significance. All analyses were performed using the Statistical Package for the Social Sciences (SPSS) software (Version 13.0; SPSS, Inc., Chicago, IL, USA). P value <0.05 was considered statistically significant.

Results

Effect of Sub-chronic DOPET Treatment on oA42i-Induced Spatial Cognitive Decrements in Mice

To explore the potential of DOPET in reversing the spatial reference and working memory impairments in oA42i-induced cognitive dysfunction, the mice were treated with DOPET and examined by using RAM. Mice in the oA42i group showed significantly ($P < 0.05$) increased memory errors (RME—2.1-fold; correct working memory error—1.6 fold; incorrect working memory error—1.9-fold) in locating the food bait, when compared to the sham-operated group (Fig. 3a–c). We observed a significant ($P < 0.05$) improvement in the correct choice and error reduction in the DOPET treated mice, compared to the oA42i group (Fig. 3a–c).

Effect of DOPET Administration on the Upstream MAPK Signaling Pathways in oA42i-Induced Neurotoxicity in Mice

MAPK signaling is one of the most studied molecular mechanisms in the field of Alzheimer's disease research, due to the critical role of these pathways in regulating cytoprotective/cytotoxic processes. In our study, oA42i-intoxicated mice depicted about 1.6- and 1.7-fold decrease in the relative protein levels of p-ERK1/2/ERK1/2 and p-RSK2/RSK2, respectively, compared to the sham-operated group ($P < 0.05$) (Fig. 4a–c). On assessment of the death signaling kinases, JNK and p38, we found that the relative protein levels of p-JNK/JNK and p-p38/p38 were significantly increased to about 2.1- and 2.7-fold, respectively, in the oA42i group, when compared to the sham-operated group (Fig. 4d–f). In contrary, DOPET treated

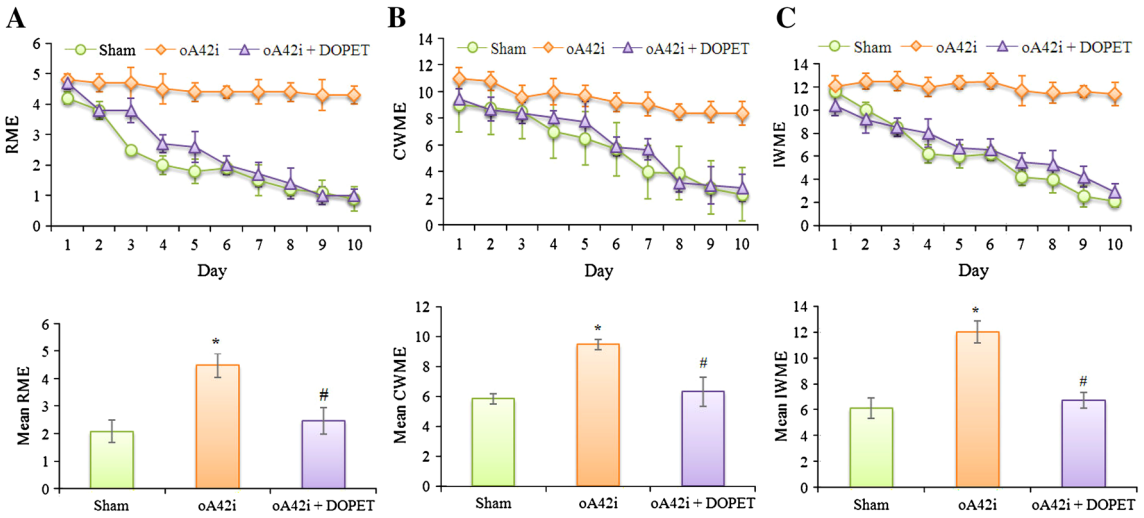

Fig. 3 Effect of DOPET on the spatial reference and working memory performances, after injecting oA42i (i.c.v.) in mice. **a** RME calculated as a function of day/group; **b** CWME calculated as a function of day/group; **c** IWME calculated as a function of day/group. Data were expressed as mean ± SD ($n = 10$ per group). $^{*}P < 0.05$ (oA42i vs control); $^{\#}P < 0.05$ (DOPET plus oA42i vs oA42i alone)

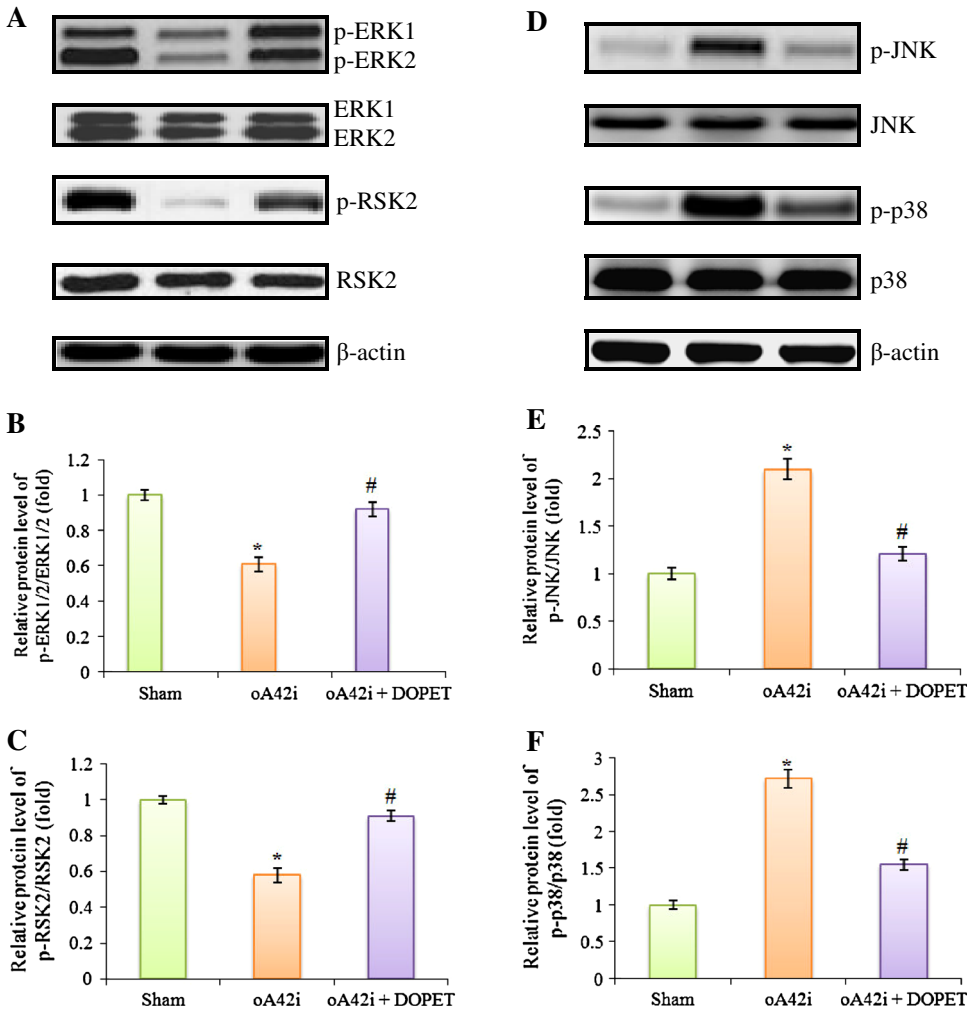

Fig. 4 Effect of DOPET on the relative phosphorylated/total MAPK protein levels in the hippocampi, 14 days after injecting oA42i (i.c.v.) in mice. **a** Representative Western blots of phosphorylated- and total-ERK1/2 and RSK2 expressions. **b** Relative protein level of p-ERK1/2 (Thr202/Tyr204)/ERK1/2. **c** Relative protein level of p-RSK2 (Thr577)/RSK2. **d** Representative Western blots of phosphorylated- and total-JNK and -p38 expressions. **e** Relative protein level of p-JNK (Thr183)/JNK. **f** Relative protein level of p-p38 (Thr180/Tyr182)/p38. Data were expressed as mean ± SD from six independent experiments with the similar results. $^{*}P < 0.05$ (oA42i vs control); $^{\#}P < 0.05$ (DOPET plus oA42i vs oA42i alone)

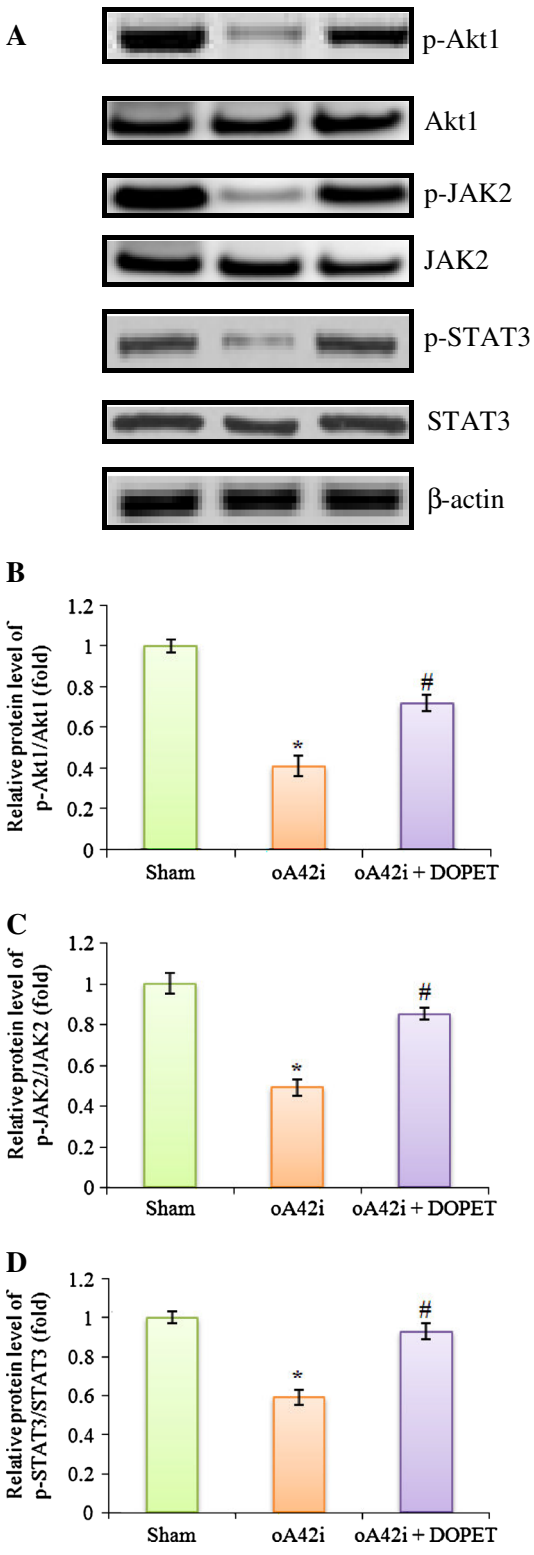

◀**Fig. 5** Effect of DOPET on the relative phosphorylated/total protein levels of Akt1, JAK2, and STAT3 in the hippocampi, 14 days after injecting oA42i (i.c.v.) in mice. **a** Representative Western blot of phosphorylated- and total-Akt1, JAK2, and STAT3 expressions. **b** Relative protein level of p-Akt1 (Ser473)/Akt1. **c** Relative protein level of p-JAK2 (Tyr1007/1008)/JAK2. **d** Relative protein level of p-STAT3 (Tyr705)/STAT3. Data were expressed as mean ± SD from six independent experiments with the similar results. $^{*}P < 0.05$ (oA42i vs control); $^{\#}P < 0.05$ (DOPET plus oA42i vs oA42i alone)

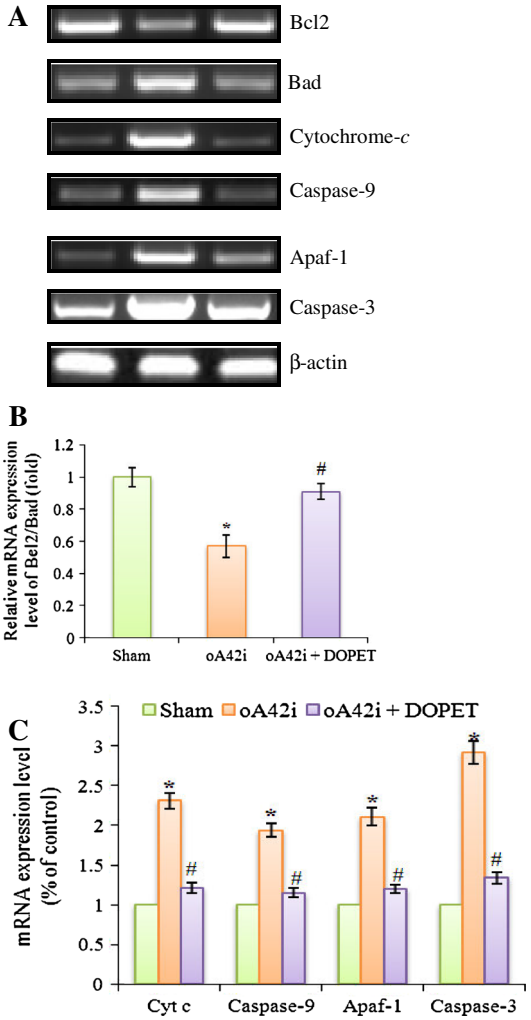

Fig. 6 Effect of DOPET on the apoptotic markers in the hippocampi, 14 days after injecting oA42i (i.c.v.) in mice. **a** Representative RT-PCR images of Bcl-2, Bad, cytochrome *c*, caspase-9, Apaf-1, and caspase-3 mRNA expressions. **b** Relative mRNA expression level of Bcl-2/Bad. **c** mRNA expression levels of cytochrome *c*, caspase-9, Apaf-1, and caspase-3. Data were expressed as mean ± SD from six independent experiments with the similar results. $^{*}P < 0.05$ (oA42i vs control); $^{\#}P < 0.05$ (DOPET plus oA42i vs oA42i alone)

mice depicted about 51 % and 57 % increase and about 42 % and 43 % decrease in the relative phosphorylated/total protein levels of ERK1/2, RSK2, JNK, and p38, respectively, compared to the oA42i group ($P < 0.05$).

Effect of DOPET Administration on the Upstream PI3K/Akt1 and JAK2/STAT3 Signaling Pathways in oA42i-Induced Neurotoxicity in Mice

PI3K/Akt1 and JAK2/STAT3 pathways play a vital role in the neuronal survival mechanisms and thus stimulation of these signaling pathways might have a beneficial role in the AD therapy. Surprisingly, we observed a marked ($P < 0.05$) 76 %, 74 %, and 59 % increase in the relative protein expression levels of p-Akt1/Akt1, p-JAK2/JAK2, and p-STAT3/STAT3, respectively, against oA42i-induced survival challenge in the hippocampal neurons. oA42i-provoked neurotoxicity caused about 2.4-, 2-, and 1.7-fold decrease ($P < 0.05$) in the relative protein expression levels of p-Akt1/Akt1, p-JAK2/JAK2, and p-STAT3/STAT3, when compared to the sham-operated group (Fig. 5a–d).

Regulatory Effect of DOPET on oA42i-Induced Hippocampal Neuronal Apoptotic Makers in Mice

With an interest to investigate the caspase-dependent mitochondria-mediated (intrinsic) apoptosis in the hippocampus, the relative mRNA expression level of Bcl-2/Bad and the mRNA expression levels of cytochrome *c*, caspase-9, Apaf-1, and caspase-3 were measured (Fig. 6a–c). oA42i group displayed about 1.8-fold decrease in the relative mRNA expression level of Bcl2/Bad and about 2.3-, 1.9-, 2.1-, and 2.9-fold increase in the mRNA expression levels of cytochrome *c*, caspase-9, Apaf-1, and caspase-3 vs sham-operated group ($P < 0.05$). On the other side, DOPET treatment caused about 60 % increase in the relative mRNA expression level of Bcl-2/Bad and about 48 %, 41 %, 43 %, and 54 % decrease in the mRNA expression levels of cytochrome *c*, caspase-9, Apaf-1, and caspase-3, respectively, vs oA42i group ($P < 0.05$).

Effect of DOPET in Modulating oA42i-Induced Dysregulation in SIRT1- and CREB-associated-Protein/mRNA Expression Levels in the Hippocampi of Mice

SIRT1 and CREB have a well-documented profile in the positive regulation of survival and memory functions in Alzheimer's disease. In our study, oA42i-induced hippocampal

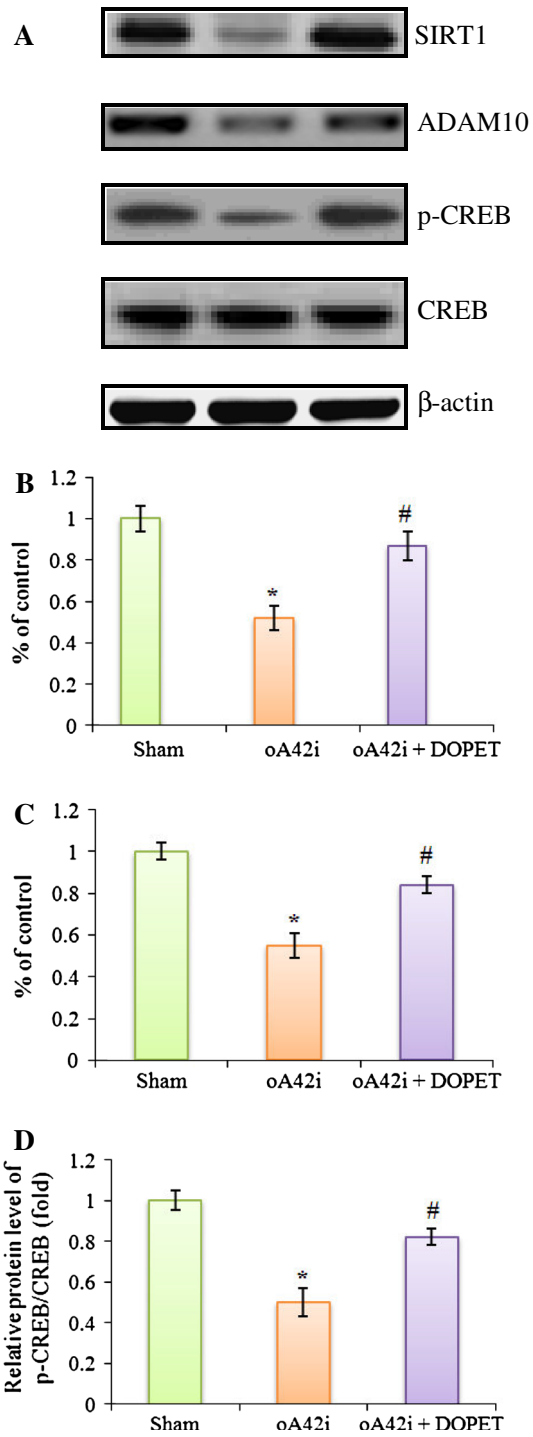

Fig. 7 Effect of DOPET on the protein expressions of SIRT1, ADAM10, and CREB in the hippocampi, 14 days after injecting oA42i (i.c.v.) in mice. **a** Representative Western blots of SIRT1, ADAM10, p-CREB, and CREB. **b** Protein level of SIRT1, as % of control. **c** Protein level of ADAM10, as % of control. **d** Relative protein level of p-CREB (Ser133)/CREB. Data were expressed as mean ± SD from three independent experiments. $^{*}P < 0.05$ (oA42i vs control); $^{\#}P < 0.05$ (DOPET plus oA42i vs oA42i alone)

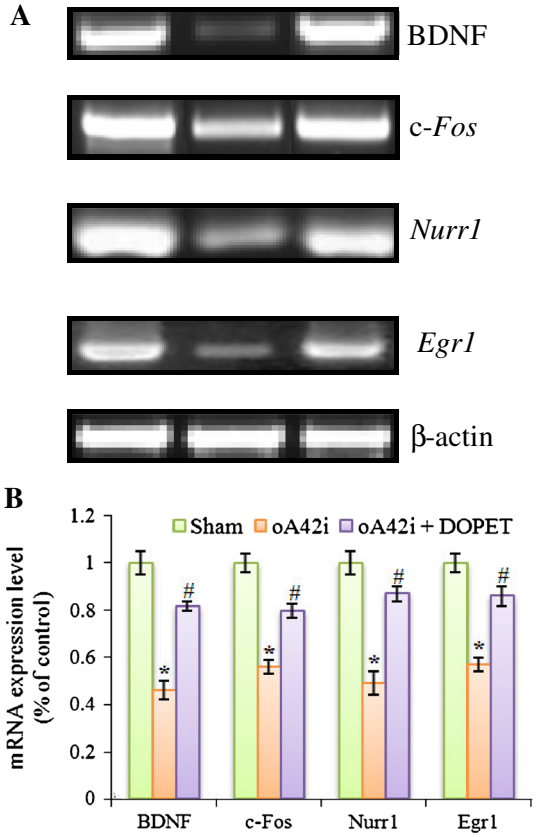

Fig. 8 Effect of DOPET on the expression of CREB-associated genes (BDNF, *c-Fos*, *Nurr1*, and *Egr1*) in the hippocampi, 14 days after injecting oA42i (i.c.v.) in mice. **a** Representative RT-PCR images of BDNF, *c-Fos*, *Nurr1*, and *Egr1*. **b** mRNA expression levels of BDNF, *c-Fos*, *Nurr1*, and Egr1. Data were expressed as mean ± SD from six independent experiments with the similar results. $^{*}P < 0.05$ (oA42i vs control); $^{\#}P < 0.05$ (DOPET plus oA42i vs oA42i alone)

injury was substantiated ($P < 0.05$) by the decrease in protein levels of SIRT1 and ADAM10 as well as the relative protein levels of p-CREB/CREB to about 1.9-, 1.8-, and 2-fold, respectively, in comparison with the sham-operated group. Parallel evaluation of DOPET treated mice showed significantly ($P < 0.05$) increased protein levels of SIRT1 and ADAM10 as well as the relative protein levels of p-CREB/CREB to about 67 %, 53 %, and 65 % ($P < 0.05$), respectively, compared to the oA42i group (Fig. 7a–d).

We also evaluated the mRNA expression levels of CREB-associated genes (BDNF, *c-Fos, Nurr1*, and *Egr1*) involved in the memory formation to unearth the link between oA42i-induced spatial memory deficits and the CREB-associated gene functions (Fig. 8a, b). Obviously, the mRNA expression levels of BDNF, *c-Fos*, *Nurr1*, and *Egr1* were decreased in the oA42i group to about 2.2-, 1.8-, 2.0-, and 1.8-fold, respectively, when compared to the sham-operated group ($P < 0.05$). In contrary, we found that the mRNA expression levels of *BDNF, c-Fos, Nurr1*, and *Egr1* were enhanced ($P < 0.05$) to about 79, 43, 78, and 51 %, respectively, in the DOPET treated mice against oA42i-induced neuro-cognitive dysfunction.

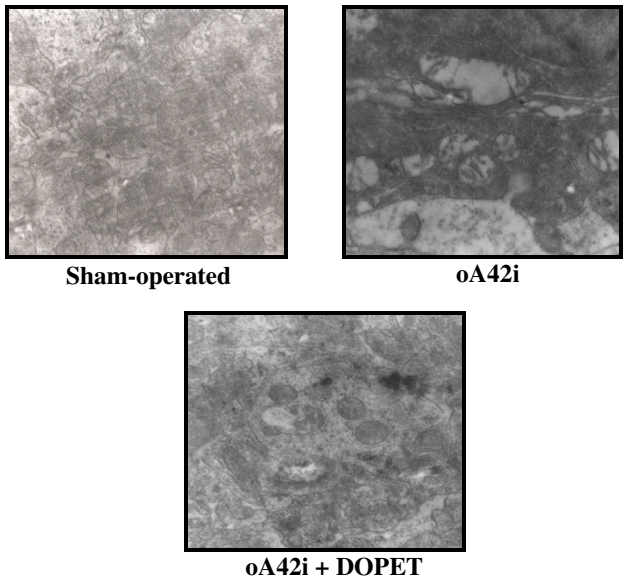

Fig. 9 Transmission electron microscopic study on the effect of DOPET (10 mg/kg/day for 14 days, p.o.) on the neuronal mitochondrial ultra-architecture, 14 days after injecting oA42i (i.c.v.) in mice

Evaluation of the Mitochondrial Protective Potential of DOPET Against oA42i-Induced Mitochondrial Aberrations by Using Transmission Electron Microscopy

Ultra-structural examination of mitochondria using transmission electron microscopy revealed a great deal of fragmentation, vacuoles, and cristae disruption in the oA42i-intoxicated mice. Besides, we observed abnormally enlarged mitochondria due to drastic mitochondrial swelling in the oA42i group. However, DOPET treatment revealed intact, healthy mitochondrial structures with clear cristae, in harmony with the ultra-architecture of the mitochondria in the hippocampal neurons of sham-operated group (Fig. 9).

Discussion

The consistency and reproducibility of amyloid beta-provoked neurotoxicity and cognitive dysfunction in the experimental models are still remaining a matter of debate in the avenue of Alzheimer's disease research. The in vivo Alzheimer's disease rodent model produced by Morimoto et al. (1998), using neurotoxic Aβ peptide (25–35) plus ibotenic acid, seems to resolve this predicament. Nevertheless,

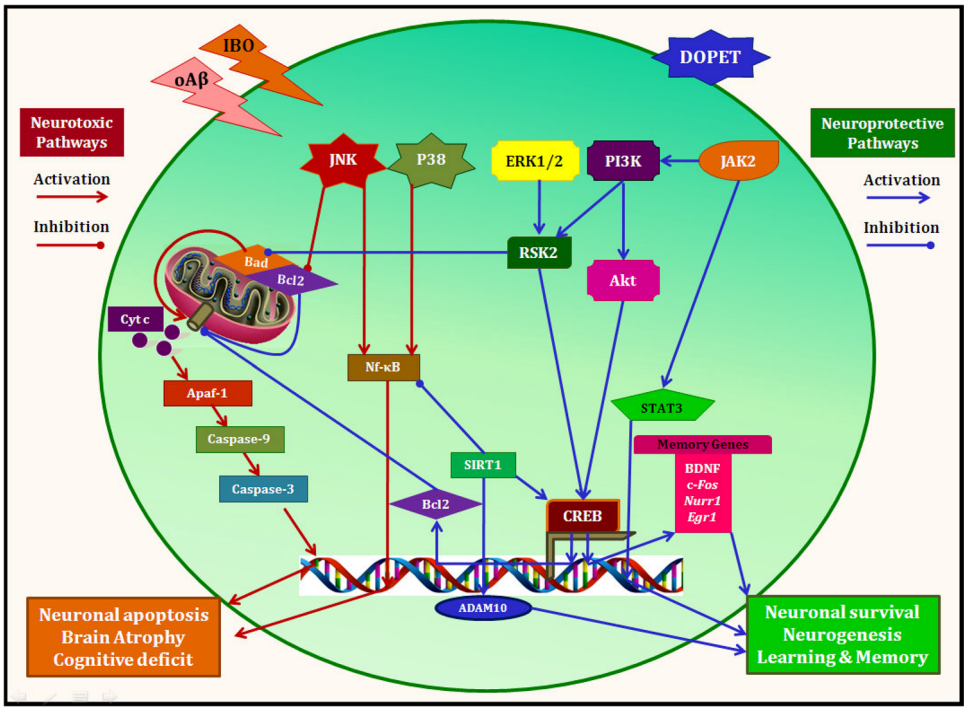

Fig. 10 Graphical representation of molecular signaling pathways involved in the neuronal survival-apoptotic programs. *DOPET* 3,4-Dihydroxyphenylethanol, *oAβ* soluble oligomeric amyloid β_{1-42} peptide, *IBO* ibotenic acid

emergence of toxic 'oligomeric Aβ hypothesis' questions the aforesaid model, as the latter is based on the outmoded 'amyloid cascade hypothesis' which fails to explain the link between deposited amyloid-β (Aβ) in plaques and progressive neuro-cognitive dysfunction (Benilova et al. 2012). In this context, we have made two simple yet influential modifications in Morimoto group's paradigm to mimic a more reliable and reproducible in vivo Alzheimer's disease model: (i) we used soluble oligomeric Aβ (oAβ) peptides, but not fibrillar Aβ (fAβ), for two key reasons—oAβ is a better neurotoxicant than fAβ or Aβ cocktail (Benilova et al. 2012); unlike fAβ, oAβ complies with the modern oligomeric Aβ hypothesis. (ii) $A\beta_{1-42}$ fragment was used in our study instead of $A\beta_{25-35}$, as the former more potently disrupts the activity of hippocampal network and associated spatial memory functions (Gutiérrez-Lerma et al. 2013; Yue et al. 2014).

In our study, mice challenged with oligomeric $A\beta_{1-42}$ plus ibotenic acid (oA42i) depicted severe impairment in the spatial reference and working memories as assessed using RAM. This outcome is in line with many earlier studies which employed $A\beta_{1-42}$ plus ibotenic acid (Hruska and Dohanich 2007), $A\beta_{40}$ plus ibotenic acid (Hu et al. 2005), or $A\beta_{25-35}$ plus ibotenic acid (Feng et al. 2012) to incite cognitive dysfunction. However, DOPET treatment at a dosage of 10 mg/(kg day) for 14 days significantly improved the spatio-cognitive performances in mice. To unravel the enigma behind the cognition-enhancing effect of DOPET, we investigated the activities of various neuromolecular signals involved in the apoptotic and survival pathways inside the hippocampal neurons.

A wealth of work has shown that three MAPK signaling pathways, namely ERK, JNK, and p38 play pivotal role in the prevention/pathogenesis of AD (Kawamata and Shimohama 2011; Kim and Choi 2010; Marwarha and Ghribi 2012). Parallel evidence on the effect of ibotenic acid revealed that ERK is inhibited in the hippocampi of intoxicated rats (Yu et al. 2012). In sync with the studies on oligomeric Aβ- or ibotenic acid-induced ERK1/2 down-regulation, our study showed that ERK1/2 activity (phosphorylation) is significantly decreased in the oA42i group, whereas treatment with DOPET increased the ERK1/2 activity similar to the level of control group.

Recent studies in the hippocampal culture (He et al. 2013; Ma et al. 2009; Zhang et al. 2014) and transgenic mouse (Sclip et al. 2011) models showed that oligomeric Aβ-induced activation of p38-MAPK and JNK-MAPK impaired the neuronal and memory functions in simulation with the pathogenic mechanisms in AD. In addition, a study showed that ibotenic acid challenge significantly upregulated the phosphorylation of p38 and JNK leading to brain cell damage (Yu et al. 2012). Our study demonstrated that DOPET treatment effectively inhibited oA42i-evoked phosphorylation of p38 and JNK, thus underscoring its positive effect against detrimental neurosignaling pathways (Fig. 10). A study in a neuroblastoma cell line demonstrated that DOPET offers neuroprotection by mitigating Aβ-induced nuclear translocation of the nuclear factor-

kappaB (NF-κB) subunits (St-Laurent-Thibault et al. 2011). This piece of evidence is tempting us to speculate that down-regulation of p38 and JNK by DOPET might have a predominant role in the decrease of both NF-κB activation and subsequent brain cell demise in the oA42i-intoxicated mice hippocampi. Of note, NF-κB was down-regulated by DOPET treatment in our study (data not shown).

Interestingly, Watson and Fan reported that amyloid β_{1-42} provoked hippocampal neuronal apoptosis is mediated by the inactivation of PI3K/Akt and ERK/RSK pathways with concomitantly activated Bad-mediated mitochondrial pore opening, followed by apoptotic neuronal death (Watson and Fan 2005). Along the lines of these findings, observations of our study revealed that oA42i-induced neuro-cognitive dysfunction is a consequence of the down-regulated PI3K/Akt and ERK1/2-RSK2/CREB survival pathways with associated Bad activation- and Bcl-2 inactivation-arbitrated apoptosis (Fig. 10). Moreover, oA42i-intoxication has triggered the caspase-dependent mitochondrial (intrinsic) apoptotic pathway that involved—the release of cytochrome *c* from the mitochondria into the cytosol as well as the activation of Apaf-1 followed by the activation of downstream initiator and executioner caspases, caspase-9, and caspase-3, respectively—finally leading to the inevitable demise of the neurons. Corresponding to this mitochondria-mediated apoptosis, a repercussion of mitochondrial failure, examination under transmission electron microscope (TEM) revealed swollen mitochondria and loss of cristae in the oA42i mice. Nevertheless, DOPET treatment significantly antagonized the negative effects of oA42i by augmenting the mitochondrial integrity, bolstering the survival signaling, and deactivating Bad-mediated apoptosis. Notably, DOPET has a well-documented mitochondrial protection profile tested across various pathological models (Schaffer et al. 2007; Signorile et al. 2014; Zhu et al. 2010).

Strategies focused on the up-regulation of genes involved in memory functions are becoming one of the most attractive areas in AD research (España et al. 2010; Gao et al. 2010). In our study, we analyzed some of the vital survival and memory genes including SIRT1 (sirtuin1; NAD^+-dependent deacetylase), CREB, and CREB-target genes (BDNF, c-*Fos*, *Nurr1*, and *Egr1*) that regulate cognitive functions. As expected, cognitive decline in the oA42i group mirrored the down-regulation of these genes in the hippocampal neurons of mice (España et al. 2010). An interesting report by Gao et al. (2010) disentangled the CREB-mediated beneficial role of SIRT1, a pro-survival gene in the spatial learning and memory functions.

We further assessed the contribution of ADAM10, a SIRT1-regulated metalloprotease gene in protecting against oA42i-induced neuro-behavioral impairment. In concurrence with the earlier reports of other researchers in neuroblastoma cell line, primary hippocampal cultures and transgenic mouse models of beta-amyloid-mediated toxicity, we found that ADAM10 activity is compromised in the oA42i-intoxicated group (Epis et al. 2008; Wang et al. 2012). Surprisingly, DOPET treatment efficiently alleviated the attenuation of ADAM10 expression, thereby advocating its robust neuroprotective effects. The increased expression of SIRT1 and CREB by DOPET alone or DOPET-rich extract was already reported in previous studies (Bayram et al. 2012; Signorile et al. 2014). As SIRT1 activation further elicited the α-secretase gene ADAM10, it could be inferred that DOPET might stimulate the non-amyloidogenic cleavage of amyloid-β protein precursor (AβPP) and enhance the clearance of neurotoxic Aβ peptide, so as to protect the hippocampal neurons. Many studies suggested that Aβ peptides induce tau phosporylation which in turn produces cytoskeletal disruption and neuritic dystrophy in the hippocampal neurons (Jin et al. 2011; Sáez et al. 2006). In this context, the ability of DOPET to inhibit tau aggregation (Daccache et al. 2011) is an evidence for the direct anti-tau effect of DOPET.

Conclusion

On the whole, our study outcome demonstrates the versatile potential of DOPET in the management of Alzheimer's disease through its potential to alleviate aberrant apoptosis-survival mechanisms that underlie neurodegeneration and cognitive impairment in AD. Nonetheless, further studies on DOPET are imperative to explicate the comprehensive mechanisms involved in the anti-amyloidogenic and anti-tauopathic effects in AD. More to the point, we deem that future research on the potential of DOPET in mitigating the expression of AD-linked genes and stimulating the longevity- and cognition-enhancing genes to enhance neuroregeneration is highly inevitable to validate the therapeutic efficacy of this putative anti-AD drug candidate.

Conflict of interest The authors declare no potential conflict of interest.

References

Auñon-Calles D, Canut L, Visioli F (2013) Toxicological evaluation of pure hydroxytyrosol. Food Chem Toxicol 55:498–504

Bayram B, Ozcelik B, Grimm S, Roeder T, Schrader C, Ernst IM, Wagner AE, Grune T, Frank J, Rimbach G (2012) A diet rich in olive oil phenolics reduces oxidative stress in the heart of SAMP8 mice by induction of Nrf2-dependent gene expression. Rejuvenation Res 15:71–81

Benilova I, Karran E, De Strooper B (2012) The toxic Aβ oligomer and Alzheimer's disease: an emperor in need of clothes. Nat Neurosci 15:349–357

Brown RW, Beale KS, Jay Frye GD (2002) Mecamylamine blocks enhancement of reference memory but not working memory produced by post-training injection of nicotine in rats tested on the radial arm maze. Behav Brain Res 134:259–265

Cao K, Xu J, Zou X, Li Y, Chen C, Zheng A, Li H, Li H, Szeto IM, Shi Y, Long J, Liu J, Feng Z (2014) Hydroxytyrosol prevents diet-induced metabolic syndrome and attenuates mitochondrial abnormalities in obese mice. Free Radic Biol Med 67:396–407

Capasso G, Di Gennaro CI, Della Ragione F, Manna C, Ciarcia R, Florio S, Perna A, Pollastro RM, Damiano S, Mazzoni O, Galletti P, Zappia V (2008) In vivo effect of the natural antioxidant hydroxytyrosol on cyclosporine nephrotoxicity in rats. Nephrol Dial Transplant 23:1186–1195

Chiba T, Yamada M, Sasabe J, Terashita K, Shimoda M, Matsuoka M, Aiso S (2009) Amyloid-beta causes memory impairment by disturbing the JAK2/STAT3 axis in hippocampal neurons. Mol Psychiatry 14:206–222

Daccache A, Lion C, Sibille N, Gerard M, Slomianny C, Lippens G, Cotelle P (2011) Oleuropein and derivatives from olives as Tau aggregation inhibitors. Neurochem Int 58:700–707

de la Puerta R, Ruiz Gutierrez V, Hoult JR (1999) Inhibition of leukocyte 5-lipoxygenase by phenolics from virgin olive oil. Biochem Pharmacol 57:445–449

de la Torre R, Covas MI, Pujadas MA, Fitó M, Farré M (2006) Is dopamine behind the health benefits of red wine? Eur J Nutr 45:307–310

Denner LA, Rodriguez-Rivera J, Haidacher SJ, Jahrling JB, Carmical JR, Hernandez CM, Zhao Y, Sadygov RG, Starkey JM, Spratt H, Luxon BA, Wood TG, Dineley KT (2012) Cognitive enhancement with rosiglitazone links the hippocampal PPARγ and ERK MAPK signaling pathways. J Neurosci 32:16725–16735

Epis R, Marcello E, Gardoni F, Longhi A, Calvani M, Iannuccelli M, Cattabeni F, Canonico PL, Di Luca M (2008) Modulatory effect of acetyl-L-carnitine on amyloid precursor protein metabolism in hippocampal neurons. Eur J Pharmacol 597:51–56

España J, Valero J, Miñano-Molina AJ, Masgrau R, Martín E, Guardia-Laguarta C, Lleó A, Giménez-Llort L, Rodríguez-Alvarez J, Saura CA (2010) Beta-amyloid disrupts activity-dependent gene transcription required for memory through the CREB coactivator CRTC1. J Neurosci 30:9402–9410

Feng C, Zhang C, Shao X, Liu Q, Qian Y, Feng L, Chen J, Zha Y, Zhang Q, Jiang X (2012) Enhancement of nose-to-brain delivery of basic fibroblast growth factor for improving rat memory impairments induced by co-injection of β-amyloid and ibotenic acid into the bilateral hippocampus. Int J Pharm 423:226–234

Fiocchetti M, De Marinis E, Ascenzi P, Marino M (2013) Neuroglobin and neuronal cell survival. Biochim Biophys Acta 1834:1744–1749

Gao J, Wang WY, Mao YW, Gräff J, Guan JS, Pan L, Mak G, Kim D, Su SC, Tsai LH (2010) A novel pathway regulates memory and plasticity via SIRT1 and miR-134. Nature 466:1105–1109

Godoy JA, Rios JA, Zolezzi JM, Braidy N, Inestrosa NC (2014) Signaling pathway cross talk in Alzheimer's disease. Cell Commun Signal 12:23

González-Correa JA, Navas MD, Lopez-Villodres JA, Trujillo M, Espartero JL, De La Cruz JP (2008) Neuroprotective effect of hydroxytyrosol and hydroxytyrosol acetate in rat brain slices subjected to hypoxia-reoxygenation. Neurosci Lett 446:143–146

González-Santiago M, Martín-Bautista E, Carrero JJ, Fonollá J, Baró L, Bartolomé MV, Gil-Loyzaga P, López-Huertas E (2006) One-month administration of hydroxytyrosol, phenolic antioxidant present in olive oil, to hyperlipemic rabbits improves blood lipid profile, antioxidant status and reduces atherosclerosis development. Atherosclerosis 188:35–42

Granados-Principal S, El-Azem N, Pamplona R, Ramirez-Tortosa C, Pulido-Moran M, Vera-Ramirez L, Quiles JL, Sanchez-Rovira P, Naudí A, Portero-Otin M, Perez-Lopez P, Ramirez-Tortosa M (2014) Hydroxytyrosol ameliorates oxidative stress and mitochondrial dysfunction in doxorubicin-induced cardiotoxicity in rats with breast cancer. Biochem Pharmacol 90:25–33

Gutiérrez-Lerma AI, Ordaz B, Peña-Ortega F (2013) Amyloid Beta peptides differentially affect hippocampal theta rhythms in vitro. Int J Pept 2013:328140

Hagiwara K, Goto T, Araki M, Miyazaki H, Hagiwara H (2011) Olive polyphenol hydroxytyrosol prevents bone loss. Eur J Pharmacol 662:78–84

Hajibagheri MAN (1999) Methods in molecular biology: electron microscopy methods and protocols, vol 117. Humana Press, Totowa

He N, Jin WL, Lok KH, Wang Y, Yin M, Wang ZJ (2013) Amyloid-β(1-42) oligomer accelerates senescence in adult hippocampal neural stem/progenitor cells via formylpeptide receptor 2. Cell Death Dis 4:e924

Hruska Z, Dohanich GP (2007) The effects of chronic estradiol treatment on working memory deficits induced by combined infusion of beta-amyloid (1–42) and ibotenic acid. Horm Behav 52:297–306

Hu Y, Xia Z, Sun Q, Orsi A, Rees D (2005) A new approach to the pharmacological regulation of memory: Sarsasapogenin improves memory by elevating the low muscarinic acetylcholine receptor density in brains of memory-deficit rat models. Brain Res 1060:26–39

Jin M, Shepardson N, Yang T, Chen G, Walsh D, Selkoe DJ (2011) Soluble amyloid beta-protein dimers isolated from Alzheimer cortex directly induce Tau hyperphosphorylation and neuritic degeneration. Proc Natl Acad Sci USA 108:5819–5824

Kawamata J, Shimohama S (2011) Stimulating nicotinic receptors trigger multiple pathways attenuating cytotoxicity in models of Alzheimer's and Parkinson's diseases. J Alzheimers Dis 24(Suppl 2):95–109

Kayed R, Lasagna-Reeves CA (2013) Molecular mechanisms of amyloid oligomers toxicity. J Alzheimers Dis 33(Suppl 1):S67–S78

Kim EK, Choi EJ (2010) Pathological roles of MAPK signaling pathways in human diseases. Biochim Biophys Acta 1802:396–405

Klein WL (2002) Abeta toxicity in Alzheimer's disease: globular oligomers (ADDLs) as new vaccine and drug targets. Neurochem Int 41:345–352

Lee-Huang S, Huang PL, Zhang D, Lee JW, Bao J, Sun Y, Chang YT, Zhang J, Huang PL (2007) Discovery of small-molecule HIV-1 fusion and integrase inhibitors oleuropein and hydroxytyrosol: Part I. fusion (corrected) inhibition. Biochem Biophys Res Commun 354:872–878

Liao FF, Xu H (2009) Insulin signaling in sporadic Alzheimer's disease. Sci Signal 2:pe36

Ma QL, Yang F, Rosario ER, Ubeda OJ, Beech W, Gant DJ, Chen PP, Hudspeth B, Chen C, Zhao Y, Vinters HV, Frautschy SA, Cole GM (2009) Beta-amyloid oligomers induce phosphorylation of tau and inactivation of insulin receptor substrate via c-Jun N-terminal kinase signaling: suppression by omega-3 fatty acids and curcumin. J Neurosci 29:9078–9089

Marwarha G, Ghribi O (2012) Leptin signaling and Alzheimer's disease. Am J Neurodegener Dis 1:245–265

Morimoto K, Yoshimi K, Tonohiro T, Yamada N, Oda T, Kaneko I (1998) Co-injection of beta-amyloid with ibotenic acid induces synergistic loss of rat hippocampal neurons. Neuroscience 84:479–487

Nehlig A (2013) The neuroprotective effects of cocoa flavanol and its influence on cognitive performance. Br J Clin Pharmacol 75:716–727

Pan S, Liu L, Pan H, Ma Y, Wang D, Kang K, Wang J, Sun B, Sun X, Jiang H (2013) Protective effects of hydroxytyrosol on liver ischemia/reperfusion injury in mice. Mol Nutr Food Res 57:1218–1227

Paxinos G, Franklin KBJ (2001) The Mouse Brain in Stereotaxic Coordinates, 2nd edn. Elsevier, New York

Praticò D (2013) Alzheimer's disease and the quest for its biological measures. J Alzheimers Dis 33(Suppl 1):S237–S241

Ristagno G, Fumagalli F, Porretta-Serapiglia C, Orrù A, Cassina C, Pesaresi M, Masson S, Villanova L, Merendino A, Villanova A, Cervo L, Lauria G, Latini R, Bianchi R (2012) Hydroxytyrosol attenuates peripheral neuropathy in streptozotocin-induced diabetes in rats. J Agric Food Chem 60:5859–5865

Rouissi K, Hamrita B, Kouidi S, Messai Y, Jaouadi B, Hamden K, Medimegh I, Ouerhani S, Cherif M, Elgaaied AB (2011) In vivo prevention of bladder urotoxicity: purified hydroxytyrosol ameliorates urotoxic effects of cyclophosphamide and buthionine sulfoximine in mice. Int J Toxicol 30:419–427

Sáez ET, Pehar M, Vargas MR, Barbeito L, Maccioni RB (2006) Production of nerve growth factor by beta-amyloid-stimulated astrocytes induces p75NTR-dependent tau hyperphosphorylation in cultured hippocampal neurons. J Neurosci Res 84:1098–1106

Satoh Y, Endo S, Ikeda T, Yamada K, Ito M, Kuroki M, Hiramoto T, Imamura O, Kobayashi Y, Watanabe Y, Itohara S, Takishima K (2007) Extracellular signal-regulated kinase 2 (ERK2) knockdown mice show deficits in long-term memory; ERK2 has a specific function in learning and memory. J Neurosci 27:10765–10776

Schaffer S, Podstawa M, Visioli F, Bogani P, Müller WE, Eckert GP (2007) Hydroxytyrosol-rich olive mill wastewater extract protects brain cells in vitro and ex vivo. J Agric Food Chem 55:5043–5049

Schmitt WB, Deacon RM, Seeburg PH, Rawlins JN, Bannerman DM (2003) A within-subjects, within-task demonstration of intact spatial reference memory and impaired spatial working memory in glutamate receptor-A-deficient mice. J Neurosci 23:3953–3959

Sclip A, Antoniou X, Colombo A, Camici GG, Pozzi L, Cardinetti D, Feligioni M, Veglianese P, Bahlmann FH, Cervo L, Balducci C, Costa C, Tozzi A, Calabresi P, Forloni G, Borsello T (2011) c-Jun N-terminal kinase regulates soluble Aβ oligomers and cognitive impairment in AD mouse model. J Biol Chem 286:43871–43880

Signorile A, Micelli L, De Rasmo D, Santeramo A, Papa F, Ficarella R, Gattoni G, Scacco S, Papa S (2014) Regulation of the biogenesis of OXPHOS complexes in cell transition from replicating to quiescent state: involvement of PKA and effect of hydroxytyrosol. Biochim Biophys Acta 1843:675–684

St-Laurent-Thibault C, Arseneault M, Longpré F, Ramassamy C (2011) Tyrosol and hydroxytyrosol, two main components of olive oil, protect N2a cells against amyloid-β-induced toxicity. Involvement of the NF-κB signaling. Curr Alzheimer Res 8:543–551

Tan YW, Zhang SJ, Hoffmann T, Bading H (2012) Increasing levels of wild-type CREB up-regulates several activity-regulated inhibitor of death (AID) genes and promotes neuronal survival. BMC Neurosci 13:48

Wang Y, Tang XC, Zhang HY (2012) Huperzine A alleviates synaptic deficits and modulates amyloidogenic and nonamyloidogenic pathways in APPswe/PS1dE9 transgenic mice. J Neurosci Res 90:508–517

Watson K, Fan GH (2005) Macrophage inflammatory protein 2 inhibits beta-amyloid peptide (1–42)-mediated hippocampal neuronal apoptosis through activation of mitogen-activated protein kinase and phosphatidylinositol 3-kinase signaling pathways. Mol Pharmacol 67:757–765

Yu X, Wang LN, Ma L, You R, Cui R, Ji D, Wu Y, Zhang CF, Yang ZL, Ji H (2012) Akebia saponin D attenuates ibotenic acid-induced cognitive deficits and pro-apoptotic response in rats: involvement of MAPK signal pathway. Pharmacol Biochem Behav 101:479–486

Yue XH, Liu XJ, Wu MN, Chen JY, Qi JS (2014) Amyloid β protein suppresses hippocampal theta rhythm and induces behavioral disinhibition and spatial memory deficit in rats. Sheng Li Xue Bao 66:97–106

Zhang LL, Sui HJ, Liang B, Wang HM, Qu WH, Yu SX, Jin Y (2014) Atorvastatin prevents amyloid-β peptide oligomer-induced synaptotoxicity and memory dysfunction in rats through a p38 MAPK-dependent pathway. Acta Pharmacol Sin. doi:10.1038/aps.2013.203

Zhao B, Ma Y, Xu Z, Wang J, Wang F, Wang D, Pan S, Wu Y, Pan H, Xu D, Liu L, Jiang H (2014) Hydroxytyrosol, a natural molecule from olive oil, suppresses the growth of human hepatocellular carcinoma cells via inactivating AKT and nuclear factor-kappa B pathways. Cancer Lett 347:79–87

Zhu L, Liu Z, Feng Z, Hao J, Shen W, Li X, Sun L, Sharman E, Wang Y, Wertz K, Weber P, Shi X, Liu J (2010) Hydroxytyrosol protects against oxidative damage by simultaneous activation of mitochondrial biogenesis and phase II detoxifying enzyme systems in retinal pigment epithelial cells. J Nutr Biochem 21:1089–1098